

Electronic Supplementary Information (ESI) for

**An anionic single-walled metal-organic nanotube with armchair
(3,3) topology as extremely smart adsorbent for effective and
selective adsorption of cationic carcinogenic dyes**

Yue Zhou, Shuo Yao, Yali Ma, Guanghua Li, Qisheng Huo, and Yunling Liu*

State Key Laboratory of Inorganic Synthesis and Preparative Chemistry, College of Chemistry, Jilin University, Changchun 130012, P. R. China.

E-mail: yunling@jlu.edu.cn; Fax: +86-431-85168624; Tel: +86-431-85168614

Materials and Methods

All starting materials and reagents were used as received from commercial sources without further purification. Elemental analyses (C, H, and N) were performed on a vario MICRO elemental analyzer. Thermal gravimetric analysis (TGA) was achieved by using a TGA Q500 thermogravimetric analyzer with a heating rate of 10 °C/min in air. Powder X-ray diffraction (PXRD) data were collected on a Rigaku D/max-2550 diffractometer with Cu-K α radiation ($\lambda = 1.5418 \text{ \AA}$). The N₂ adsorption isotherm was measured using a Micromeritics ASAP 2040 instrument at 77 K under 1 bar. The infrared spectra (IR) were recorded on a Bruker IFS-66v/S FTIR spectrometer in the range of 400-4000 cm⁻¹ using the KBr pallet. The liquid state UV-vis spectra were performed on a SHIMADZU UV-2450 UV-visible spectrophotometer by using the same solvent as the blank.

Synthesis of [CH₃NH₃][Zn(NTB)(NMF)]·4.5NMF (JLU-MONT1)

Single crystals of **JLU-MONT1** were prepared by solvothermal reaction of Zn(NO₃)₂·6H₂O (12 mg, 0.04 mmol) and 4,4',4''-nitrilotrisbenzoic acid (H₃NTB, 15 mg, 0.04 mmol) in the mixture of *N*-methylformamide (NMF, 1 mL) and deionized water (0.35 mL) at 115 °C for 3 days. The colorless hexagonal prism-shaped crystals were generated and washed with *N,N*-dimethylformamide (DMF), then dried in air (yield 55% based on H₃NTB). Elemental analysis (%) calcd for **JLU-MONT1**: C 49.75, H 5.76, N 13.19; found: C 49.42, H 5.91, N 13.03.

Single-Crystal X-ray Crystallography

Crystallographic data of as-synthesized **JLU-MONT1** was collected on a Bruker Apex II CCD diffractometer using graphite-monochromated Mo K α ($\lambda = 0.71073 \text{ \AA}$) radiation at room temperature. The structure of **JLU-MONT1** was solved by direct method and refined by full-matrix least-squares on F^2 using SHELXTL program.^[1] The zinc atoms were located first, and then the carbon, nitrogen and oxygen atoms of the crystals were subsequently found in difference Fourier maps. All the non-hydrogen atoms were refined with anisotropic displacement parameters. The hydrogen atoms were located geometrically with isotropic parameters. Topology information for **JLU-MONT1** was determined by TOPOS 4.0.^[2] The final formula of **JLU-MONT1** was designated from the crystallographic data combined with thermogravimetric and elemental analysis data. The summary crystal data and structure refinements for **JLU-MONT1** were presented in Table S1, and the selective bond lengths and angles as well as the hydrogen bond data of the compound were given in Tables S2 and S3. The supplementary crystallographic data for **JLU-MONT1** (CCDC number 1573784) can be obtained free of charge from the Cambridge Crystallographic Data Centre upon request at www.ccdc.cam.ac.uk/data_request/cif.

N₂ Adsorption

Before gas adsorption measurement, the as-synthesized **JLU-MONT1** (80 mg) was dried at room temperature and then activated by using the ‘outgas’ function of the surface area analyzer for 10 h at 30 °C.

Dye Adsorption and Separation

All the experiments were performed on freshly prepared **JLU-MONT1** (10 mg) in DMF solution under consecutive stirring in dark condition and at room temperature. Different shaped and charged organic dyes, namely, basic red 9 (BR9), basic violet 14 (BV14), methyl violet (MV), rhodamine 6G (Rh6G), methylene blue (MLB) as cationic dyes, neutral red (NR) as neutral dye, and methyl orange (MO) as anionic dye, were used to test the abilities of adsorption and separation for **JLU-MONT1**. For adsorption experiments, the as-synthesized **JLU-MONT1** was transferred into the dye solutions (20 mL, 10 ppm), respectively. The concentrations of dyes were recorded by measuring the intensity of maximum absorption peak *via* UV-vis spectrophotometer at a pre-determined time. According to the different adsorption performances, binary mixtures of BR9&NR, BR9&MO, BV14&NR, BR14&MO, MV&NR and MV&MO in 1:1 molar ratios (20 mL, 10 ppm) were selected to assess the selectivity of **JLU-MONT1**. The maximum adsorption amounts for cationic dyes BR9, BV14, MV, Rh6G, and MLB were investigated in 100 mL dye solutions with different initial concentrations for 24 h. The amounts of absorbed dyes at time Q_t and at equilibrium Q_e were calculated as follows:^[3]

$$Q_t = (C_0 - C_t) V / m \quad (1)$$

$$Q_e = (C_0 - C_e) V / m \quad (2)$$

in which C₀, C_t and C_e are the concentrations of dyes at initial, time, and equilibrium, respectively. V is the volume of the dye solutions and m is the mass of **JLU-MONT1**.

To keep the accuracy of maximum adsorption amounts, three groups of repeated experiments were performed simultaneously, and the final adsorption uptakes are the average values.

Structure Description

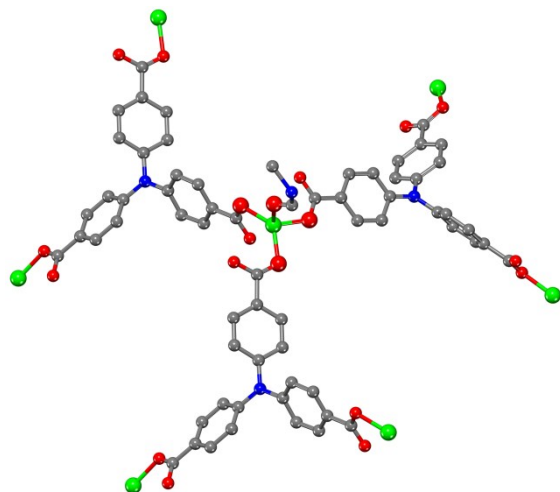


Fig. S1 Coordination environment of the Zn ions and organic ligands (all hydrogen atoms and solvent molecules are omitted for clarity).

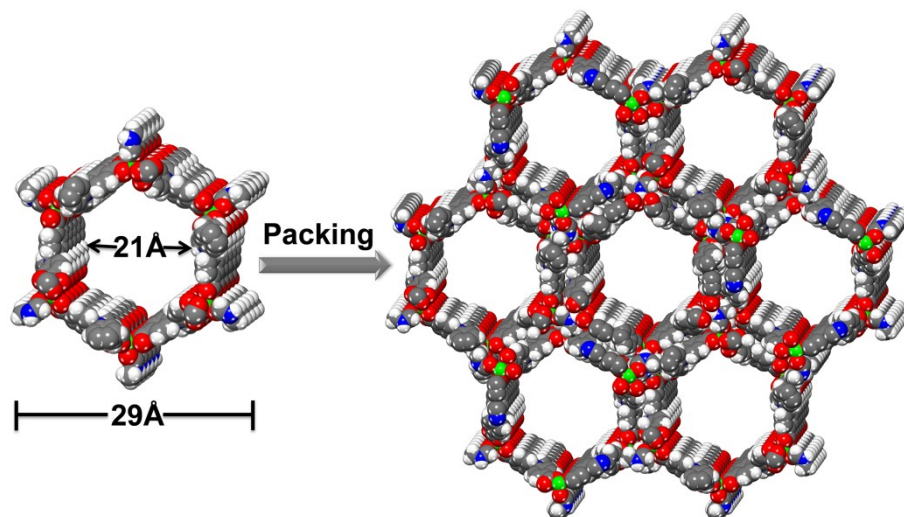


Fig. S2 Top view of the hollow nanotube with an exterior wall diameter of 29 Å and an interior channel diameter of 21 Å regardless of van der Waals radius.

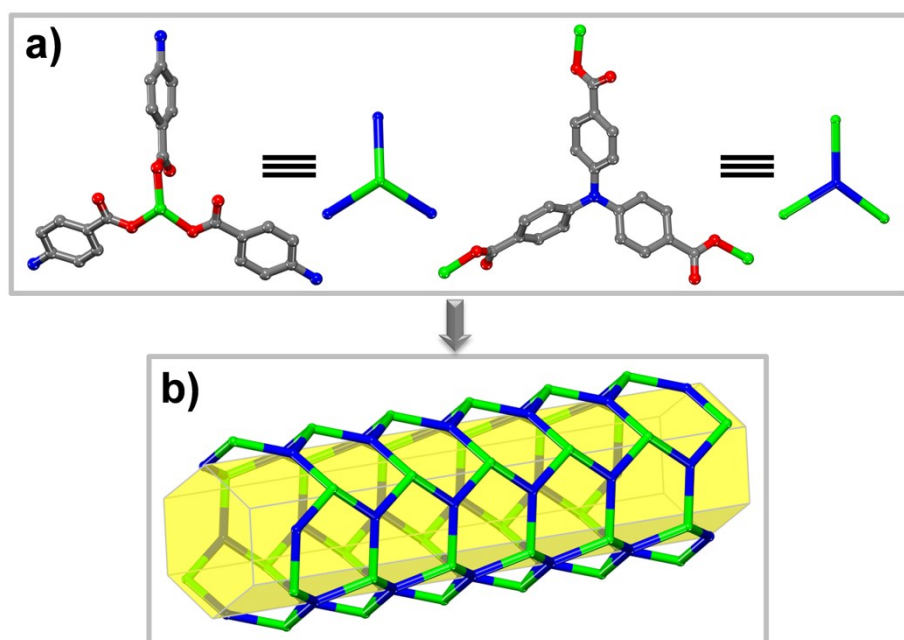


Fig. S3 Topology analysis of discrete nanotube in **JLU-MONT1**: (a) zinc center and NTB ligand can be simplified as the 3-connected nodes, respectively; (b) side view of the 1D nanotube with the yellow hexagonal prism representing the channel.

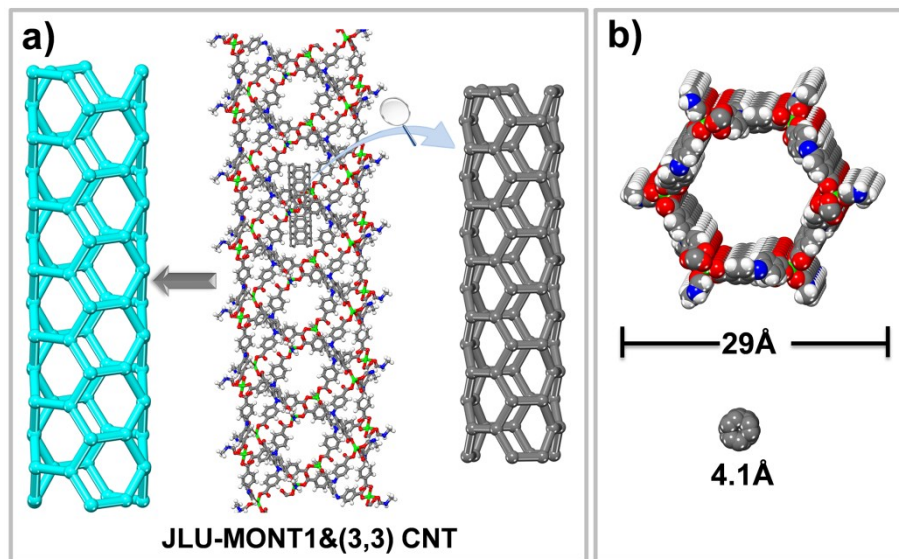


Fig. S4 Topology (a) and size (b) comparison of the discrete nanotube in **JLU-MONT1** with single-walled carbon nanotube with (3,3) index.

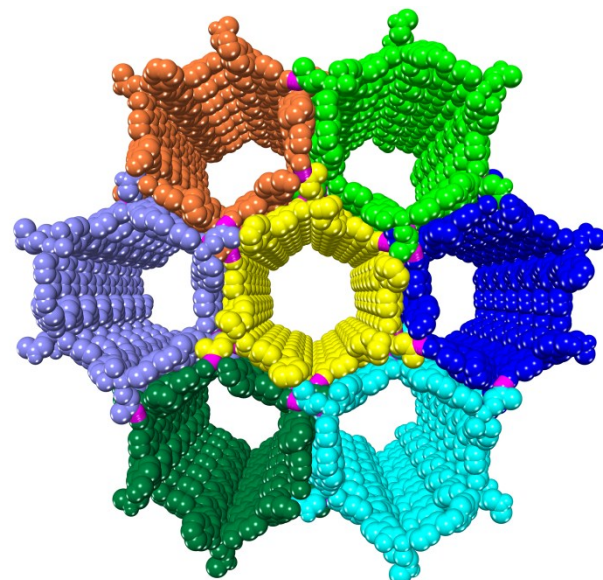


Fig. S5 Space-filling view of **JLU-MONT1** (pink balls represent the hydrogen-bonds).

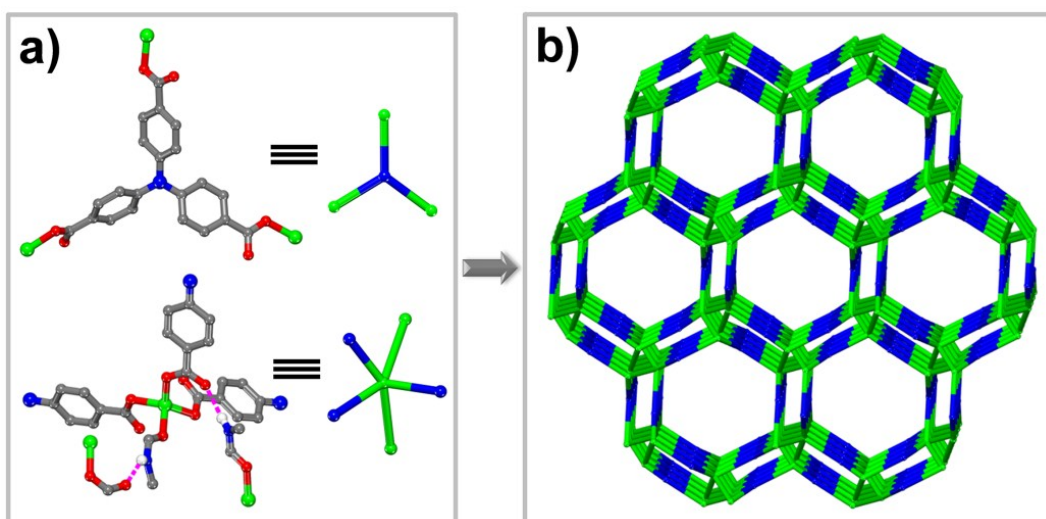


Fig. S6 Topology analysis of **JLU-MONT1**: (a) H₃NTB ligand can be simplified as a 3-connected node, and zinc unit can be seen as a 5-connected node considering hydrogen-bonds; (b) topology of **JLU-MONT1** along [001] direction.

Spectra Characterization

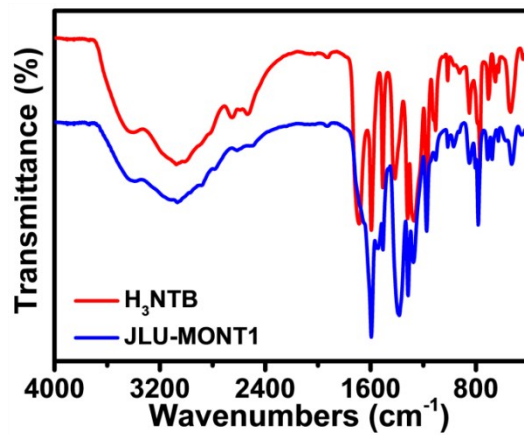


Fig. S7 FT-IR spectra of H_3NTB and **JLU-MONT1**.

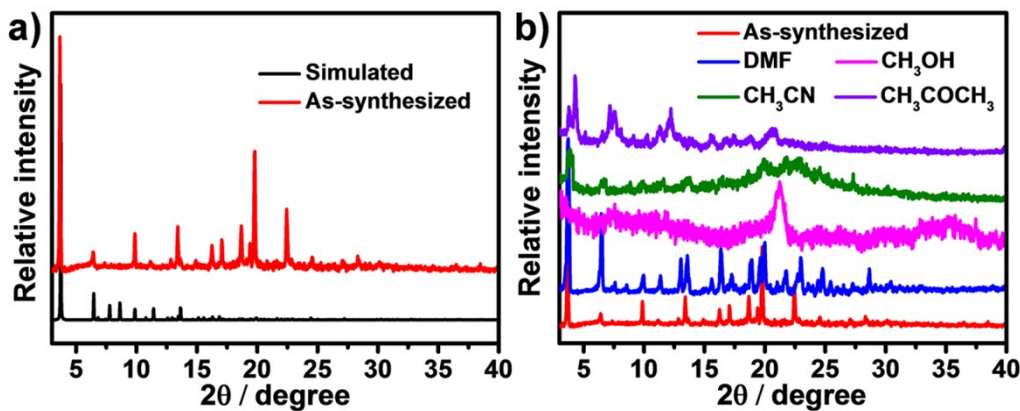


Fig. S8 PXRD patterns of (a) simulated and as-synthesized as well as (b) DMF, CH_3OH , CH_3CN , and CH_3COCH_3 soaked **JLU-MONT1** samples.

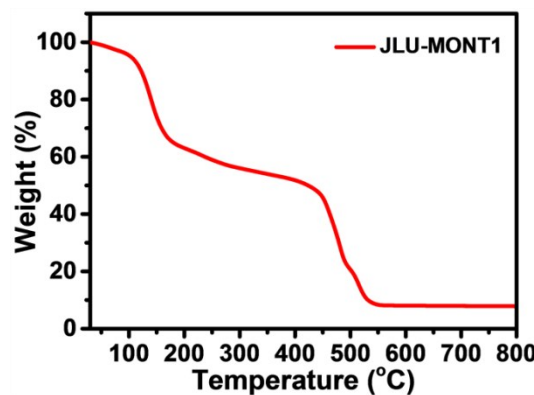


Fig. S9 TGA curve for **JLU-MONT1**.

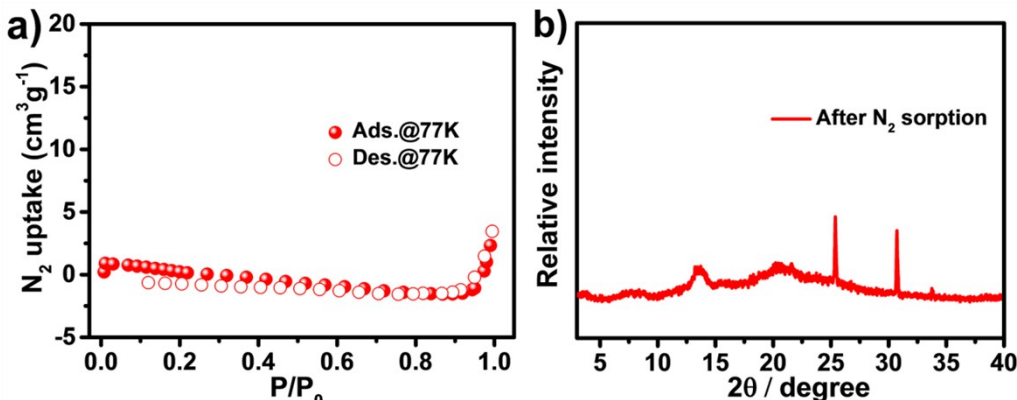


Fig. S10 (a) N_2 sorption isotherm at 77 K under 1 bar and (b) PXRD pattern after N_2 sorption for **JLU-MONT1**.

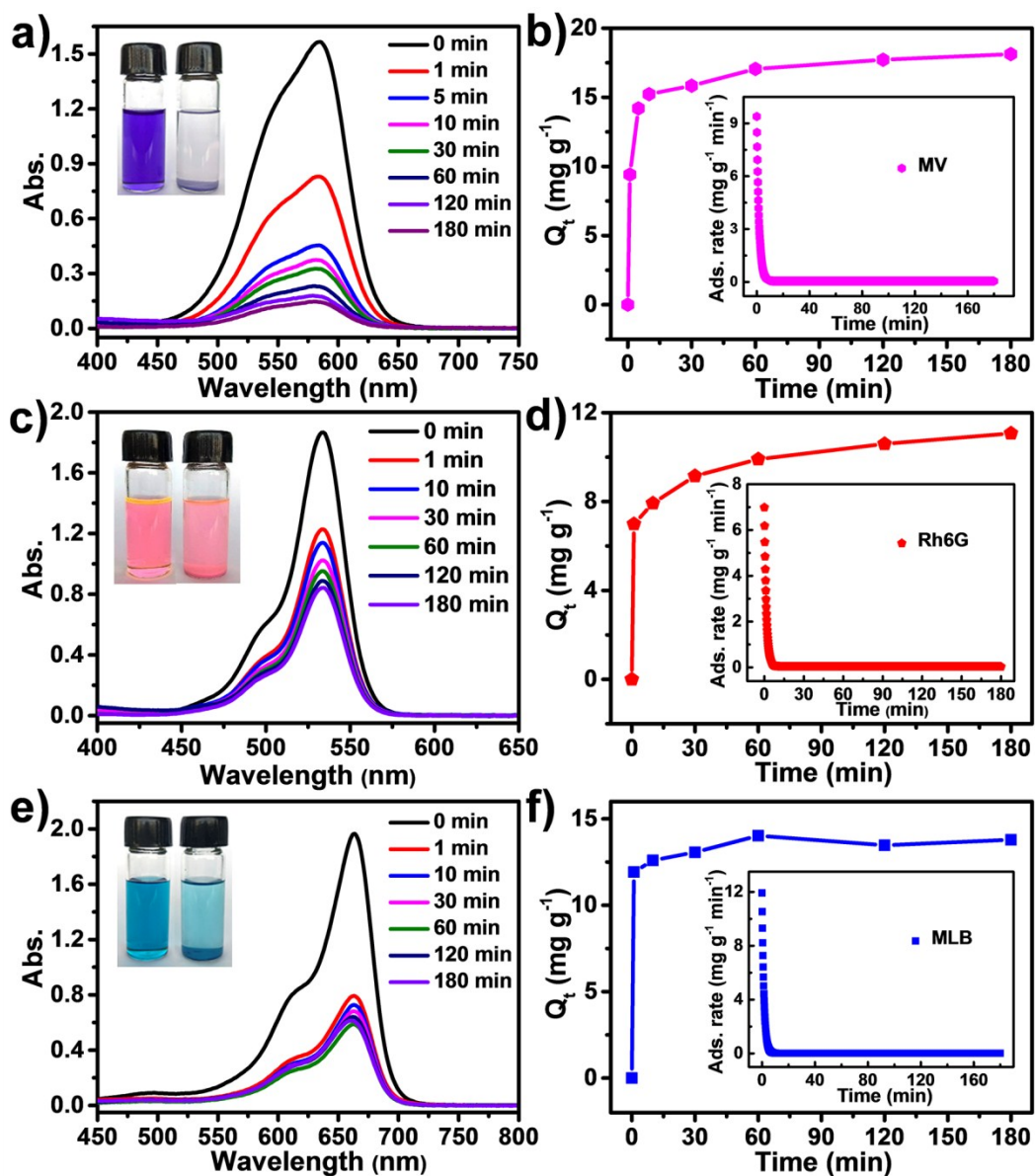


Fig. S11 UV-vis spectra of MV (a), Rh6G (c), and MLB (e) show the adsorption processes with **JLU-MONT1** at different times, the inset profiles display the change of color before (left) and after (right) adsorption; the variable adsorption amounts (Q_t) and corresponding first-order derivative curves with time for MV (b), Rh6G (d), and MLB (f).

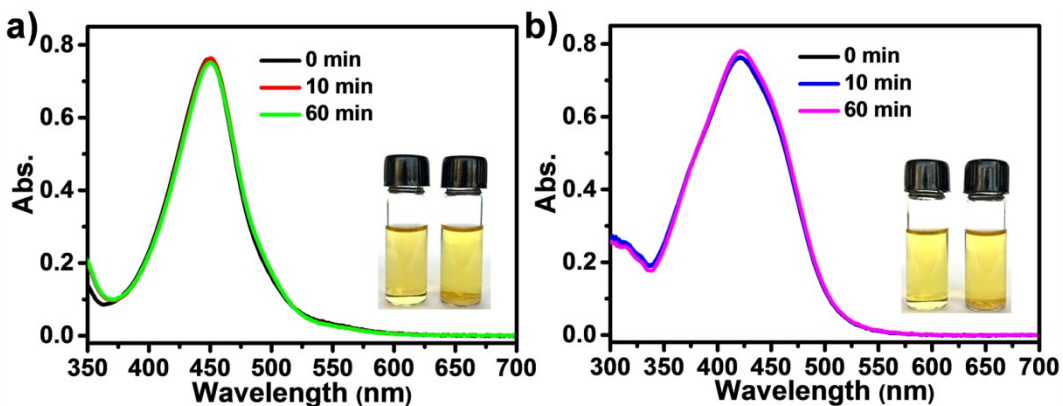


Fig. S12 UV-vis spectra of NR (a) and MO (b) show the adsorption processes with **JLU-MONT1** at different times, the inset profiles display the change of color before (left) and after (right) adsorption.

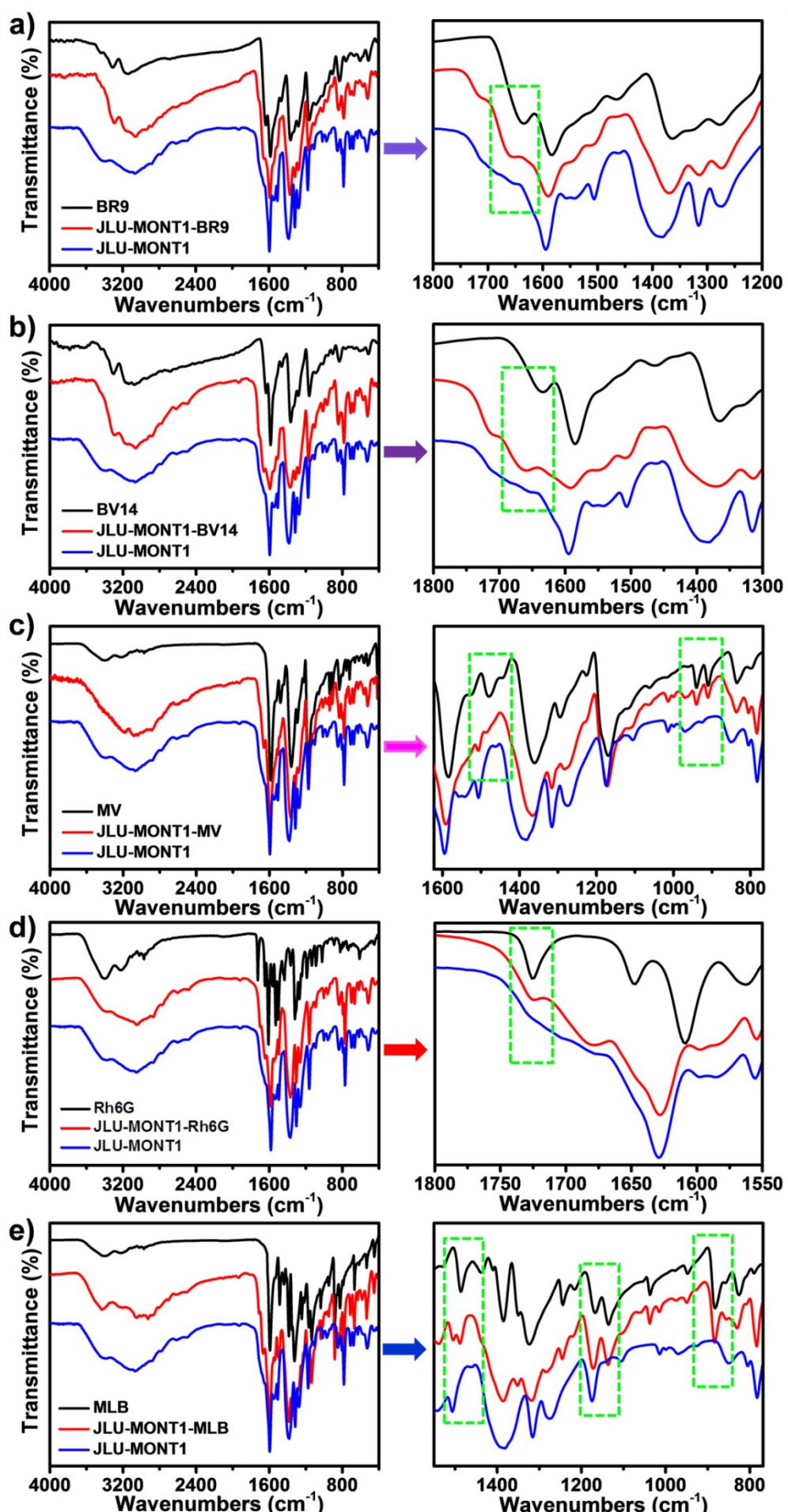


Fig. S13 FT-IR spectra of dyes, dye-adsorbed samples and **JLU-MONT1** for BR9 (a), BV14 (b), MV (c), Rh6G (d), and MLB (e).

FT-IR spectroscopy has been used to monitor the successful adsorption of BR9, BV14, MV, Rh6G, and MLB molecules for **JLU-MONT1**. As shown above, the obvious characteristic absorption peaks of corresponding cationic dyes were emerged after encapsulated in the channels of **JLU-MONT1**.

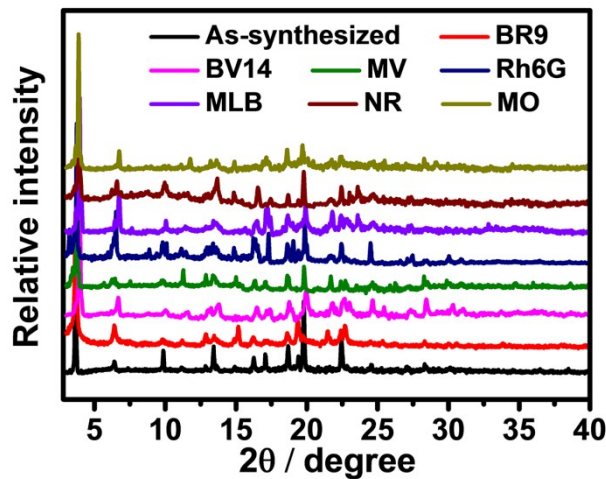


Fig. S14 PXRD patterns of as-synthesized and dye-adsorbed samples for **JLU-MONT1**.

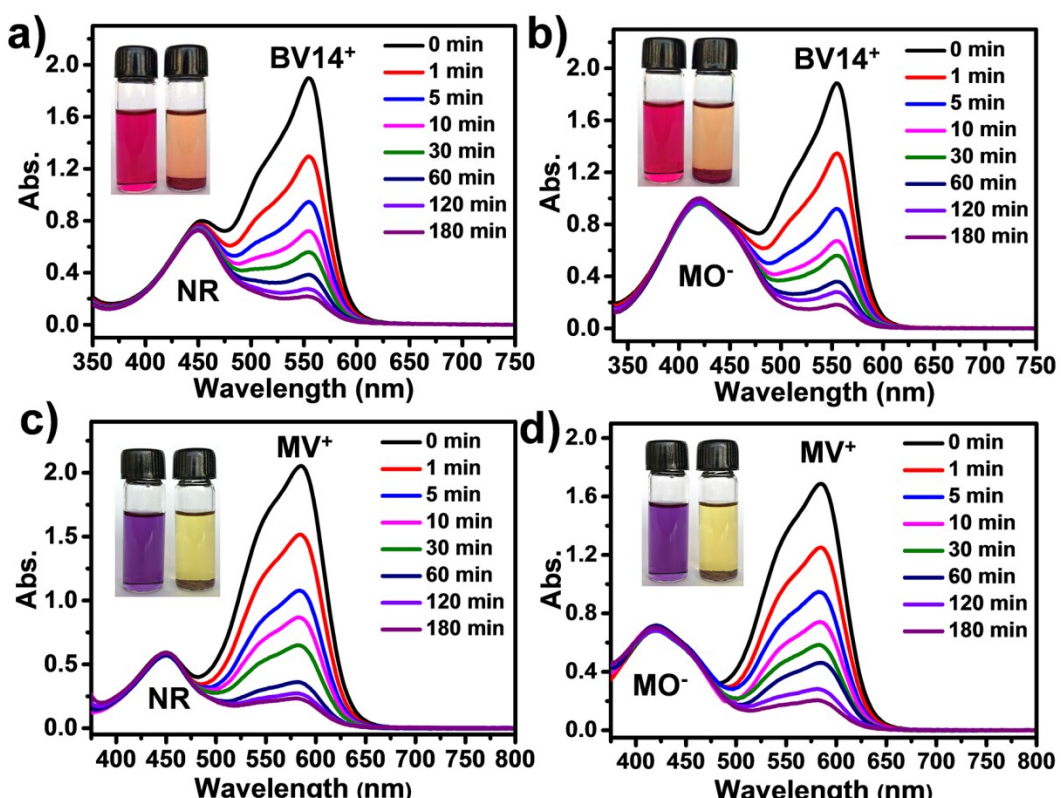


Fig. S15 UV-vis spectra for the mixtures of BV14&NR (a), BV14&MO (b), MV&NR (c), and MV&MO (d) with **JLU-MONT1** at different times, the inset profiles display the change of color before (left) and after (right) adsorption.

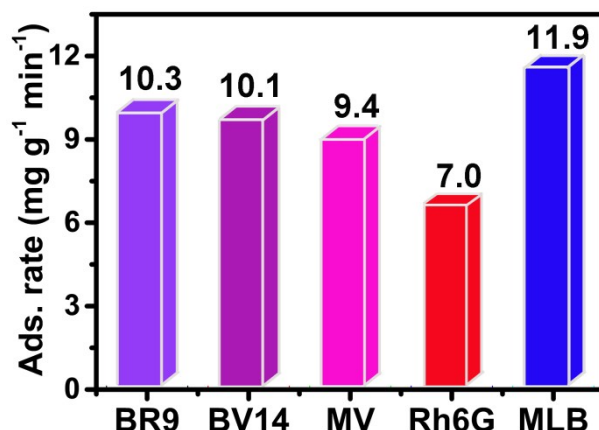


Fig. S16 The initial adsorption rates of BR9, BV14, MV, Rh6G, and MLB based on first-order derivative.

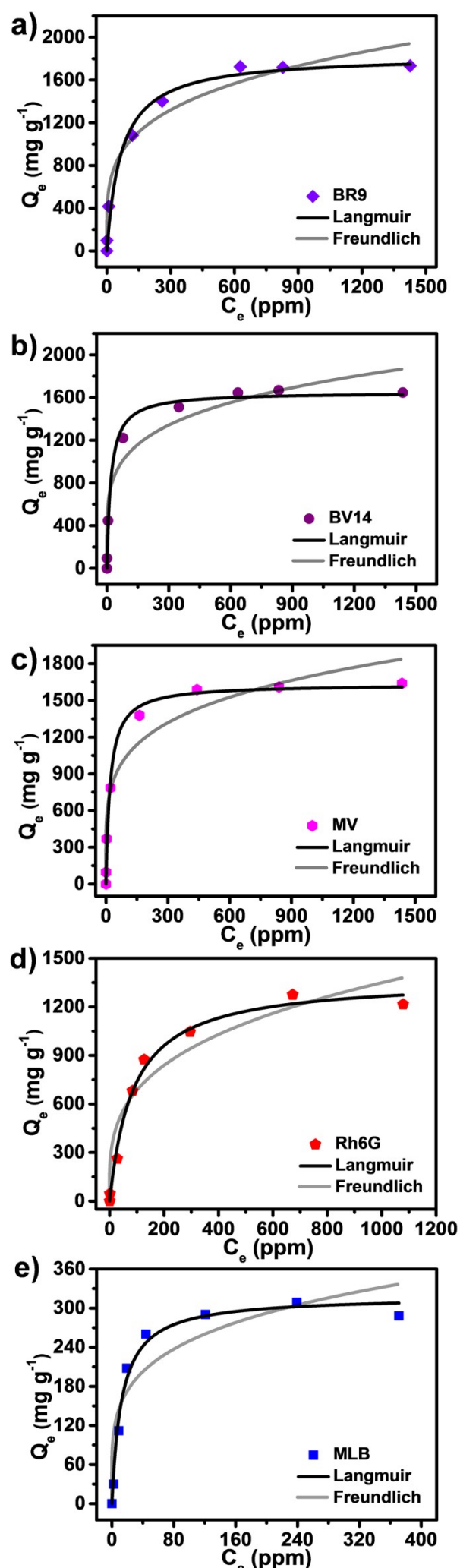


Fig. S17 Langmuir and Freundlich isotherms fitting plots for the adsorption of BR9 (a), BV14 (b), MV (c), Rh6G (d), and MLB (e).

Scheme S1 Space-filling modes of dyes@JLU-MONT1, (a) BR9, (b) BV14, (c) MV, (d) Rh6G, and (e) MLB.

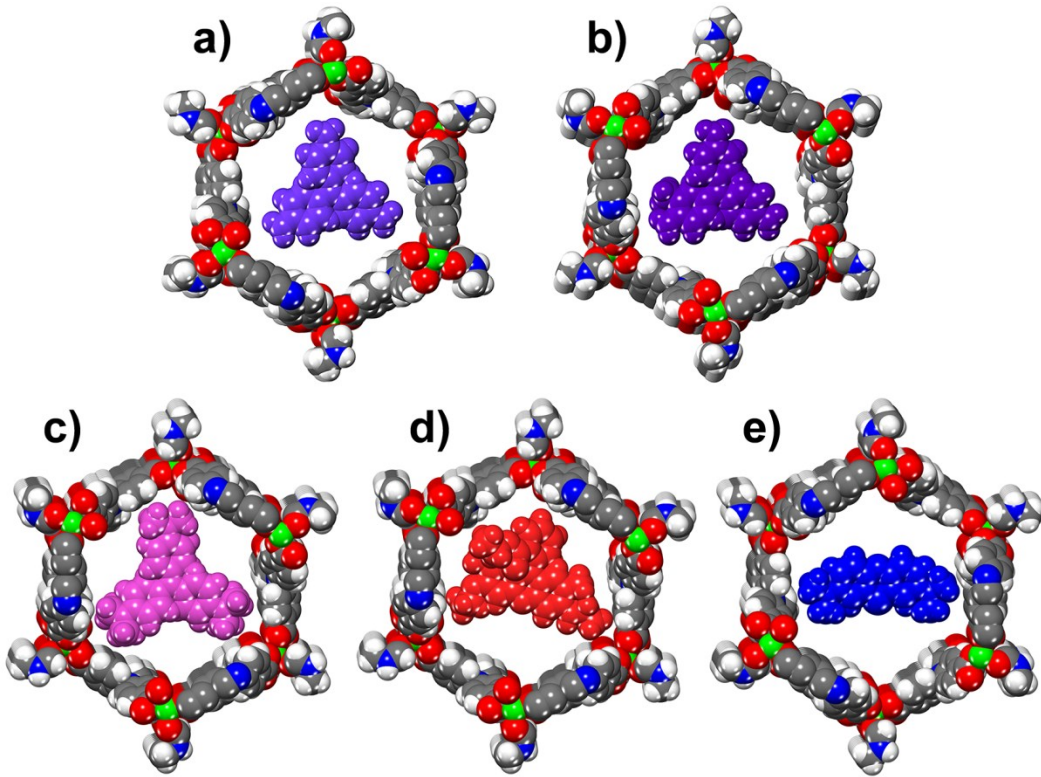


Table S1 Crystal data and structure refinement for **JLU-MONT1**.

compound	JLU-MONT1
formula	C ₃₃ H _{45.5} N _{7.5} O _{11.5} Zn
formula weight	796.64
temperature (K)	293(2)
wavelength (Å)	0.71073
crystal system	trigonal
space group	R-3
<i>a</i> (Å)	47.432(7)
<i>b</i> (Å)	47.432(7)
<i>c</i> (Å)	13.658(3)
α (°)	90
β (°)	90
γ (°)	120
volume (Å ³)	26611(7)
<i>Z</i> , <i>D_c</i> (Mg/m ³)	18, 0.895
<i>F</i> (000)	7524
θ range (deg)	1.49-25.06
reflns collected/unique	57781/10467
<i>R</i> _{int}	0.0848
data/restraints/params	10467/36/307
GOF on <i>F</i> ²	0.930
<i>R</i> _I , <i>wR</i> ₂ (<i>I</i> >2σ(<i>I</i>))	0.0661, 0.1745
<i>R</i> _I , <i>wR</i> ₂ (all data)	0.1215, 0.1925

$$R_I = \sum |F_o| - |F_c| / \sum |F_o|. \quad wR_2 = [\sum [w(F_o^2 - F_c^2)^2] / \sum [w(F_o^2)^2]]^{1/2}$$

Table S2 Selected bond lengths (\AA) and angles ($^{\circ}$) for **JLU-MONT1**.

Zn(1)-O(1)	1.942(3)	Zn(1)-O(5)#1	1.962(3)
Zn(1)-O(3)#2	1.977(3)	Zn(1)-O(7)	2.007(3)
O(3)-Zn(1)#3	1.977(3)	O(5)-Zn(1)#4	1.962(3)
O(1)-Zn(1)-O(5)#1	97.56(13)	O(1)-Zn(1)-O(3)#2	119.16(12)
O(5)#1-Zn(1)-O(3)#2	130.96(13)	O(1)-Zn(1)-O(7)	107.36(13)
O(5)#1-Zn(1)-O(7)	103.71(13)	O(3)#2-Zn(1)-O(7)	95.47(13)

Symmetry codes: #1 $y-1/3, -x+y+1/3, -z+4/3$; #2 $y-1/3, -x+y+1/3, -z+1/3$;
#3 $x-y+2/3, x+1/3, -z+1/3$; #4 $x-y+2/3, x+1/3, -z+4/3$.

Table S3 Hydrogen bond data for **JLU-MONT1**.

D-H...A	d(D-H)	d(H...A)	d(D...A)	\angle (DHA)
N(2)-H(2)...O(2)#1	0.86	2.119	2.816	137.78

Symmetry codes: #1 $-x+y-1/3, -x+1/3, z+1/3$.

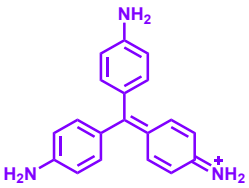
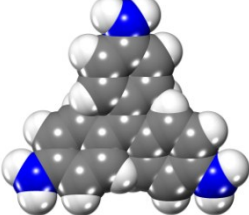
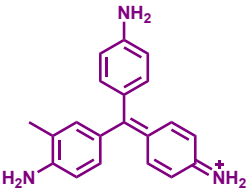
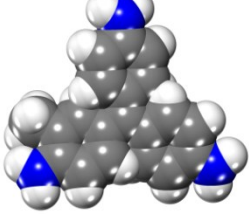
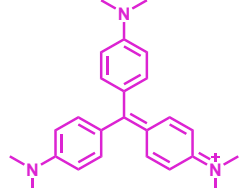
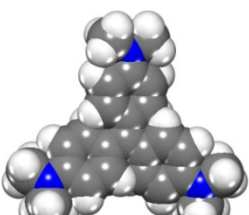
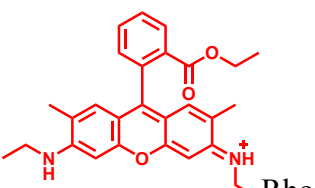
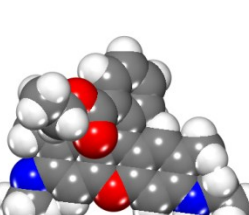
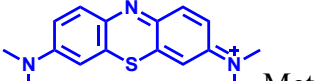
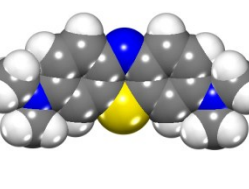
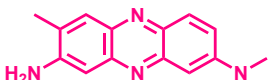
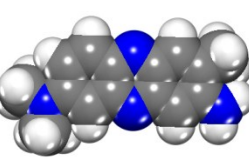
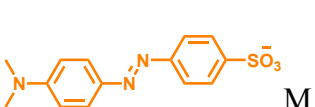
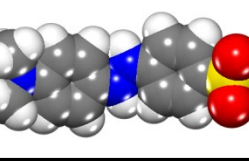
Table S4 Comparison of the primary structure features and channel diameter on the reported MONTs.

MONTs	Primary structure features	Channel diameter (\AA)	Ref.
AgLBF₄·0.5(C₆H₆)	4-connected square	8.2×12	[4]
MONT-1	4-connected square	11.2×11.2	[5]
MONT-A1	(4,4)-square sheet, (6,6) index	14.0	[6]
MONT-1	(4,4)-square sheet, chirality	12.8×13.9	[7]
[In(1,3-BDC)₂]⁻	4-connected topology	3.9	[8]
[Pt(en)(bpy)I]₄	4-connected square	5.9	[9]
(NO₃)₈·16H₂O			
[ZnLCl₂]·8H₂O	double-helices	33.2	[10]
[Mn^{II}₂Mn^{III}(L)₂(dca)₂Br₂	3-connected, (4,0) index	3.5-6.5	[11]
MMONT-5	(4,4)-square sheet, (6,0) index	24.0	[12]
Ni-TCPE1	(4,4)-square sheet	21.0	[13]
Zn(L)(H₂O)_n	3-connected , (3,3) index	10.9×6.9×15.1	[14]
2·ClO₄	hexagonal 3d-4f metallocycle	16.4	[15]
MB-1	dissectible bamboo-like tube	8.1	[16]
Zn₃(gtsp)₃	[3+3] triangular prism	2.5-2.7	[17]
Zn₄(gtsp)₄	[4+4] tetranuclear nanotubes	3.0-5.0	[17]
JLU-MONT1	3-connected, (3,3) index	21.0	This work

Table S5 The element contents of **JLU-MONT1** after heated under different temperatures.

Samples	Elemental Content [%]		
	C	H	N
JLU-MONT1-r.t.	49.42	5.91	13.03
JLU-MONT1-200 °C	53.67	4.54	7.75
JLU-MONT1-420 °C	58.16	2.31	3.02

Table S6 Molecular parameters of the dyes.^[18-20]

Dyes	Charge	Dimensions (Å)	Molecular structure with CPK mode
	+1	2.7×11.0×12.5	
Basic Red 9 (BR9)			
	+1	2.9×11.0×12.5	
Basic Violet 14 (BV14)			
	+1	3.5×13.0×13.7	
Methyl Violet (MV)			
	+1	10.9×15.7×15.8	
Rhodamine 6G (Rh6G)			
	+1	1.8×5.5×14.2	
Malachite Green (MLB)			
	0	2.3×6.4×12.6	
Neutral Red (NR)			
	-1	4.5×6.0×14.8	
M			

ethyl Orange (MO)

Table S7 The maximum adsorption amounts for BR9, BV14, MV, Rh6G, and MLB on **JLU-MONT1**, based on the data of three different batch experiments.

Cationic dyes	BR9 (mg/g)	BV14 (mg/g)	MV (mg/g)	Rh6G (mg/g)	MLB (mg/g)
Sample 1	1745	1667	1631	1241	309
Sample 2	1707	1656	1597	1271	288
Sample 3	1732	1636	1618	1263	320
Average	1725	1653	1615	1258	306

Table S8 Comparison of maximum adsorption amounts for BR9 on various adsorbents.

Adsorbent	Q _e (mg/g)	Ref.	Adsorbent	Q _e (mg/g)	Ref.
JLU-MONT1	1725	This work	Activated carbon	131	[26]
Activated carbon	428.4	[21]	Graphene-based nanocomposite	89.4	[27]
Clay	344.83	[22]	Industrial sludge	70.4	[28]
Fibers	250	[23]	AGHSB	67.11	[29]
Sunflower stalks-treated	204.6	[24]	Sepiolite	32.35	[30]
Pirina	189.3	[25]	Jalshakti	11.7	[31]
Sunflower stalks	187.32	[24]			

Table S9 Comparison of maximum adsorption amounts for BV14 on various adsorbents.

Adsorbent	Q _e (mg/g)	Ref.	Adsorbent	Q _e (mg/g)	Ref.
JLU-MONT1	1653	This work	Ca-bentonite	100	[34]
Calophyllum inophyllum Shells	1416.43	[32]	Nanofiber	67.11	[35]
Theobroma cacao Shells	980.39	[32]	Deoiled Soya	12.03	[36]
Curcuma angustifolia Scales	208.33	[33]	Bottom ash	6.39	[36]

Na-bentonite	147.9	[34]	
---------------------	-------	------	--

Table S10 Comparison of maximum adsorption amounts for MV on various adsorbents.

Adsorbent	Q _e (mg/g)	Ref.	Adsorbent	Q _e (mg/g)	Ref.
PMCS	1728.3	[37]	SAAC	85.8	[46]
JLU-MONT1	1615	This work	JLU-Liu39	84	[18]
Superporous monolith	1585	[38]	Erionite	83.8	[47]
HPP-3	699	[39]	Magnetic nanocomposite	81.7	[48]
GFP	254.2	[40]	PKF	78.9	[49]
mGO/PVA-50%	221.2	[41]	Clinoptilolite	70.7	[47]
Sr-BTTC	184	[42]	TGW	64.9	[50]
CSAC	135.1	[43]	PAAC	60.4	[46]
Opal	101.1	[44]	CPBP	32.8	[51]
TPR	94.3	[45]	WAC	19.8	[52]

Table S11 Comparison of maximum adsorption amounts for Rh6G on various adsorbents.

Adsorbent	Q _e (mg/g)	Ref.	Adsorbent	Q _e (mg/g)	Ref.
JLU-MONT1	1258	This work	GSC	55	[57]
BioNC Hydrogel	1244.7	[53]	Activated carbon	44.7	[58]
Nanoclay	428.9	[54]	Hydrogel-0.2	36.8	[59]
Chitosan	411.3	[54]	C₁₆/SiO₂-Fe₃O₄NPs	35.6	[60]
Chitosan clay	440.9	[54]	Graphene Oxide	23.3	[61]
TiP	217.4	[55]	1-min sludge	16.2	[62]
Palm shell powder	105	[56]			

Table S12 Comparison of maximum adsorption amounts for MLB on various adsorbents.

Adsorbent	Q_e (mg/g)	Ref.	Adsorbent	Q_e (mg/g)	Ref.
CTS-g-PAA/10% VMT	1685.6	[63]	Cd-MOF2	317.9	[73]
PMCS	1615.9	[37]	JLU-Liu39	308	[18]
FJI-C2	1323	[64]	JLU-MONT1	306	This work
MIL-100(Fe)	1105	[65]	Sr-BTTC	270	[42]
PCN-222	906	[66]	MIL-101(Al)	193	[67]
amino-MIL-101(Al)	762	[67]	MOF-235	187	[74]
MIL-100(Fe)	736.2	[68]	LPTNs	184	[3]
MIL-100(Cr)	643.3	[68]	Graphene	153.9	[75]
PAC2	588	[69]	CSAC	153.9	[43]
F400	476	[69]	HPP-3	144	[39]
Zn-MOF	410	[70]	Zn(phenDIB) (AOBTC)_{0.5}	139.4	[76]
DS1	401	[71]	Cd-MOF1	105	[73]
PAC1	380	[69]	Cd-MOF3	30	[73]
Peat	324.0	[72]	Zn-MOF	0.75	[77]

Reference

1. G. Sheldrick, *Acta Crystallographica Section A*, 2008, **64**, 112.
2. V. A. Blatov, A. P. Shevchenko and D. M. Proserpio, *Cryst. Growth Des.*, 2014, **14**, 3576.
3. C.-H. Lin, D. S.-H. Wong and S.-Y. Lu, *ACS Appl. Mater. Interfaces*, 2014, **6**, 16669.
4. Y.-B. Dong, Y.-Y. Jiang, J. Li, J.-P. Ma, F.-L. Liu, B. Tang, R.-Q. Huang and S. R. Batten, *J. Am. Chem. Soc.*, 2007, **129**, 4520.
5. F. Dai, H. He and D. Sun, *J. Am. Chem. Soc.*, 2008, **130**, 14064.
6. T.-T. Luo, H.-C. Wu, Y.-C. Jao, S.-M. Huang, T.-W. Tseng, Y. Wen, G.-H. Lee, S.-M. Peng and K.-L. Lu, *Angew. Chem., Int. Ed.*, 2009, **48**, 9461.
7. J.-C. Jin, Y.-Y. Wang, P. Liu, R.-T. Liu, C. Ren and Q.-Z. Shi, *Cryst. Growth Des.*, 2010, **10**, 2029.
8. F. Bu and S.-J. Xiao, *CrystEngComm*, 2010, **12**, 3385.
9. K. Otsubo, Y. Wakabayashi, J. Ohara, S. Yamamoto, H. Matsuzaki, H. Okamoto, K. Nitta, T. Uruga and H. Kitagawa, *Nat. Mater.*, 2011, **10**, 291.
10. G.-Q. Kong, S. Ou, C. Zou and C.-D. Wu, *J. Am. Chem. Soc.*, 2012, **134**, 19851.
11. G. Wu, J. Bai, Y. Jiang, G. Li, J. Huang, Y. Li, C. E. Anson, A. K. Powell and S. Qiu, *J. Am. Chem.*

Soc., 2013, **135**, 18276.

12. G.-L. Zhang, L.-P. Zhou, D.-Q. Yuan and Q.-F. Sun, *Angew. Chem., Int. Ed.*, 2015, **54**, 9844.
13. Z. Zhou, C. He, J. Xiu, L. Yang and C. Duan, *J. Am. Chem. Soc.*, 2015, **137**, 15066.
14. L. Yang, Y. Zhang, R. Lv, J. Wang, X. Fu, W. Gu and X. Liu, *CrystEngComm*, 2015, **17**, 5625.
15. J. Wu, L. Zhao, L. Zhang, X.-L. Li, M. Guo, A. K. Powell and J. Tang, *Angew. Chem., Int. Ed.*, 2016, **55**, 15574.
16. T.-W. Tseng, T.-T. Luo, S.-H. Liao, K.-H. Lu and K.-L. Lu, *Angew. Chem., Int. Ed.*, 2016, **55**, 8343.
17. B. M. Paterson, K. F. White, J. M. White, B. F. Abrahams and P. S. Donnelly, *Angew. Chem., Int. Ed.*, 2017, **56**, 8370.
18. S. Yao, T. Xu, N. Zhao, L. Zhang, Q. Huo and Y. Liu, *Dalton Trans.*, 2017, **46**, 3332.
19. Y. Song, R.-Q. Fan, K. Xing, X. Du, T. Su, P. Wang and Y.-L. Yang, *Cryst. Growth Des.*, 2017, **17**, 2549.
20. D.-M. Chen, J.-Y. Tian, Z.-W. Wang, C.-S. Liu, M. Chen and M. Du, *Chem. Commun.*, 2017, **53**, 10668.
21. K. V. Kumar, K. Porkod and F. Rocha, *J. Hazard. Mater.*, 2008, **150**, 158.
22. W. T. Tsai, Y. M. Chang, C. W. Lai and C. C. Lo, *Appl. Clay Sci.*, 2005, **29**, 149.
23. M. Arslan and M. Yiğitoğlu, *J. Appl. Polym. Sci.*, 2008, **110**, 30.
24. W. Shi, X. Xu and G. Sun, *J. Appl. Polym. Sci.*, 1999, **71**, 1841.
25. N. Mehmet, G. Ismailand and A. Bilal, *Asian J. Chem.*, 2012, **24**, 1698.
26. K. V. Kumar and S. Sivanesan, *J. Hazard. Mater.*, 2006, **129**, 147.
27. C. Wang, C. Feng, Y. Gao, X. Ma, Q. Wu and Z. Wang, *Chem. Eng. J.*, 2011, **173**, 92.
28. M. Seredych and T. J. Bandosz, *Ind. Eng. Chem. Res.*, 2007, **46**, 1786.
29. N. Sivarajasekar and R. Baskar, *J. Ind. Eng. Chem.*, 2014, **20**, 2699.
30. O. Duman, S. Tunç and T. G. Polat, *Microporous Mesoporous Mater.*, 2015, **210**, 176.
31. R. Dhodapkar, N. N. Rao, S. P. Pande, T. Nandy and S. Devotta, *React. Funct. Polym.*, 2007, **67**, 540.
32. S. Suresh, *SpringerPlus*, 2016, **5**, 633.
33. T. Maiyalagan, S. Suresh and R. S. Wilfred, *Ind. J. Chem. Technol.*, 2014, **21**, 368.
34. Y.-X. Jiang, H.-J. Xu, D.-W. Liang and Z.-F. Tong, *C. R. Chimie*, 2008, **11**, 125.
35. M. F. Elkady, M. R. El-Aassar and H. S. Hassan, *Polymer*, 2016, **8**, 177.
36. V. K. Gupta, A. Mittal, V. Gajbe and J. Mittal, *J. Colloid Interface Sci.*, 2008, **319**, 30.
37. S. Zhang, M. Zeng, J. Li, J. Li, J. Xu and X. Wang, *J. Mater. Chem. A*, 2014, **2**, 4391.
38. F. Wang, Y. Zhu, W. Wang, L. Zong, T. Lu and A. Wang, *Front. Chem.*, 2017, DOI: 10.3389/fchem.2017.00033.
39. H. Liu and H. Liu, *J. Mater. Chem. A*, 2017, **5**, 9156.
40. A. Saeeda, M. Sharifb and M. Iqbala, *J. Hazard. Mater.*, 2010, **179**, 564.
41. Z. Cheng, J. Liao, B. He, F. Zhang, F. Zhang, X. Huang and L. Zhou, *ACS Sustain. Chem. Eng.*, 2015, **3**, 1677.
42. Y. Shen, C.-C. Fan, Y.-Z. Wei, J. Du, H.-B. Zhu and Y. Zhao, *Dalton Trans.*, 2016, **45**, 10909.
43. M. Özdemir, Ö. Durmuş, Ö. Şahin and C. Saka, *Desalin. and Water Treatment*, 2016, **57**, 18038.

44. W. Ma, X. Y. Song, Y. Q. Pan, Z. H. Cheng, G. Xin, B. D. Wang and X. G. Wang, *Chem. Eng. J.*, 2012, **193**, 381.
45. C. Kannan, N. Buvaneswari and T. Palvannan, *Desalin.*, 2009, **249**, 1132.
46. S. Senthilkumaar, P. Kalaamani and C. V. Subburaam, *J. Hazard. Mater.*, 2006, **136**, 800.
47. V. Hernández-Montoya, M. A. Pérez-Cruz, D. I. Mendoza-Castillo, M. R. Moreno-Virgen and A. Bonilla-Petriciolet, *J. Environ. Manag.*, 2013, **116**, 213.
48. K. P. Singh, S. Gupta, A. K. Singh and S. Sinha, *J. Hazard. Mater.*, 2011, **186**, 1462.
49. G. O. El-Sayed, *Desalin.*, 2011, **272**, 225.
50. R. Kumar and R. Ahmad, *Desalin.*, 2011, **265**, 112.
51. R. Ahmad, *J. Hazard. Mater.*, 2009, **171**, 767.
52. R. Malarvizhi and Y.-S. Ho, *Desalin.*, 2010, 264, 97.
53. N. Kumar, H. Mittal, V. Parashar, S. S. Ray and J. C. Ngila, *RSC Adv.*, 2016, **6**, 21929.
54. A. Vanamudan and P. Pamidimukkala, *Int. J. Biol. Macromol.*, 2015, **74**, 127.
55. K. C. Maheria and U. V. Chudasama, *Ind. Eng. Chem. Res.*, 2007, **46**, 6852.
56. G. Sreelatha and P. Padmaja, *Am. J. Environ. Prot.*, 2008, **2**, 63.
57. S. S. Gupta, T. S. Sreeprasad, S. M. Maliyekkal, S. K. Das and T. Pradeep, *ACS Appl. Mater. Interfaces*, 2012, **4**, 4156.
58. G. Annadurai, R. S. Juang and D. J. Lee, *J. Environ. Sci. Health, Part A: Toxic/Hazard. Subst. Environ. Eng.*, 2001, **36**, 715.
59. A. Vanamudan, K. Bandwala and P. Pamidimukkala, *Int. J. Biol. Macromol.*, 2014, **69**, 506.
60. Y.-P. Chang, C.-L. Ren, Q. Yang, Z.-Y. Zhang, L.-J. Dong, X.-G. Cheng and D.-S. Xue, *Appl. Surf. Sci.*, 2011, **257**, 8610.
61. H. Ren, D. D. Kulkarni, R. Kodiyath, W. Xu, I. Choi and V. V. Tsukruk, *ACS Appl. Mater. Interfaces*, 2014, **6**, 2459.
62. G. Annadurai, R. S. Juang, P. S. Yen and D. J. Lee, *Adv. Environ. Res.*, 2003, **7**, 739.
63. Y. Liu, Y. Zheng and A. Wang, *J. Environ. Sci.*, 2010, **22**, 486.
64. X.-S. Wang, J. Liang, L. Li, Z.-J. Lin, P. P. Bag, S.-Y. Gao, Y.-B. Huang and R. Cao, *Inorg. Chem.*, 2016, **55**, 2641.
65. F. Tan, L. Min, K. Li, Y. Wang, J. Wang, X. Guo, G. Zhang and C. Song, *Chem. Eng. J.*, 2015, **281**, 360.
66. H. Li, X. Cao, C. Zhang, Q. Yu, Z. Zhao, X. Niu, X. Sun, Y. Liu, L. Ma and Z. Li, *RSC Adv.*, 2017, **7**, 16273.
67. E. Haque, V. Lo, A. I. Minett, A. T. Harris, T. L. Church, *J. Mater. Chem. A*, 2014, **2**, 193.
68. M. Tong, D. Liu, Q. Yang, S. Devautourvinot, G. Maurin and C. Zhong, *J. Mater. Chem. A*, 2013, **1**, 8534.
69. E. N. E. Qada, S. J. Allen and G. M. Walker, *Chem. Eng. J.*, 2008, **135**, 174.
70. S. Kumar, G. Verma, W.-Y. Gao, Z. Niu, L. Wojtas and S. Ma, *Eur. J. Inorg. Chem.*, 2016, **27**, 4373.
71. K. V. Kumar and S. Sivanesan, *J. Hazard. Mater.*, 2006, **134**, 237.
72. A. N. Fernandes, C. A. P. Almeida, C. T. B. Menezes, N. A. Debacher and M. M. D. Sierra, *J. Hazard. Mater.*, 2007, **144**, 412.
73. F.-Y. Yi, J.-P. Li, D. Wu and Z.-M. Sun, *Chem.-Eur. J.*, 2015, **21**, 11475.
74. E. Haque, J. W. Jun and S. H. Jhung, *J. Hazard. Mater.*, 2011, **185**, 507.
75. T. Liu, Y. Li, Q. Du, J. Sun, Y. Jiao, G. Yang, Z. Wang, Y. Xia, W. Zhang, K. Wang, H. Zhu and D. Wu, *Colloids Surf. B*, 2012, **90**, 197.
76. M.-K. Wu, F.-Y. Yi, Y. Fang, X.-W. Xiao, S.-C. Wang, L.-Q. Pan, S.-R. Zhu, K. Tao and L. Han, *Cryst. Growth Des.*, 2017, **17**, 5458.
77. C. Y. Sun, X. L. Wang, C. Qin, J. L. Jin, Z. M. Su, P. Huang and K. Z. Shao, *Chem.-Eur. J.*, 2013, **19**, 3639.